Annales
Geophysicae
Discussions

Intermediate Layers responses to Geomagnetic Activity During the 2009 Deep Solar Minimum Over the Brazilian Low Latitude Sector

Ângela M. Santos[1], Christiano G. M. Brum[2], Inez S. Batista[1], José H. A. Sobral[1], Mangalathayil A. Abdu[1], and Jonas R. Souza[1]

1National Institute for Space Research, São José dos Campos, Brazil.

2Arecibo Observatory, University of Central Florida, Arecibo, Puerto Rico.

Correspondence to: Ângela Santos (angelamacsantos@gmail.com; angelasantos_1@yahoo.com.br)

Abstract. Intermediate layers (ILs) are regions of enhanced electron density located in the ionospheric valley that extends from the peak altitude of the daytime E-region to the bottom side of the F-region. This work presents the daytime behavior of the ILs parameters (the virtual height - h'IL, and the top frequency - ftIL) over the low latitude region of Cachoeria Paulista (CP, 22.42° S; 45° W, I: -34.4°) for the deepest solar minimum of the last 500 years. In such a unique condition, this research reveals for the first time the ILs' quiet state seasonal behavior as well as its responses to moderate changes in the geomagnetic activity. The main results show that even small variations of geomagnetic activity (quantified by the planetary Kp index) are able to modify the dynamics of the ILs parameters. For the first time, it was observed that during the summer, the h'IL decrease rapidly with the increase of geomagnetic activity mainly in the early morning hours. In the following hours, a smoothed rise of the IL was found in all seasons analyzed. Regarding to frequency, it was observed that after 12:00 LT, there is a tendency of it decreased with the increase of the magnetic disturbances, being this characteristic more intense after 16:00 LT, except in the equinox, when little or no response was found during all the interval analyzed. In addition, it stands out that the annual periodicity of the ftIL was observed while the h'IL presents semiannual component.

1 Introduction

The deep solar minimum of the solar cycle 23/24 provides an unprecedented opportunity to understand the variability of Earth's ambient ionosphere. During this period, an unusually inactive state

of the Sun with only relatively small sunspot-carrying active regions was observed. The solar fluxes (UV, EUV, and X-rays) responsible for the heating of the upper atmosphere and production of the ionosphere

30   and the well-known 10.7 cm solar radio flux (F10.7cm) presented very low values when compared to the previous solar cycle (see for example Balan et al., 2012 and Kutiev et al., 2013).

Great efforts have been made to better understand the behavior of the different ionospheric layers over the equatorial and low latitudes sectors during this period that was considered the deepest solar minimum of the last 500 years (Hady, 2013). In this context, the effects caused by geomagnetic activities

35   are highlighted, since the variability of radiation coming from the Sun in this case can be neglected. Liu et al. (2012), for example, discussed the impacts of the high-speed stream in the equatorial ionization anomaly (EIA) development. They showed that the inhibition in the EIA formation was probably due to a westward disturbance dynamo electric field. Santos et al. (2016) investigated the behavior of the equatorial F region zonal and vertical plasma drifts over Jicamarca during the weak geomagnetic storm

40   of June 2008. Based on a realistic low-latitude ionospheric model (SUPIM - Sheffield University Plasmasphere-Ionosphere Model), they showed that the perfect anti-correlation between the vertical and the zonal drifts close to the evening prereversal enhancement of the zonal electric field was driven mainly by a vertical Hall electric field induced by the primary zonal electric field in the presence of an enhanced nighttime E region ionization (see Abdu et al., 1998). Sreeja et al. (2011), in their turn, showed that the

45   daytime E-region westward drift over Trivandrum (8.5°N, 77°E; dip latitude ~0.5°N) presented a reduction that was simultaneous with the disappearance of the equatorial sporadic E layer (E_{sq}) echoes in the ionograms. In this case, it was suggested that an additional overshielding electric field (westward/eastward during the day/night), superposed on the ionosphere during the storm main phase contributed to the observed reduction in the drift.

50   While the effects of the geomagnetic storms on the E, F, and sporadic-E (Es) layers are widely investigated, little information can be found about such effects on those layers located in the ionospheric valley, especially during the deep solar cycle minimum of 2008-2009. These layers, which are known as "intermediate layers (or just ILs)" are defined as a region of enhanced electron density located in the ionospheric valley that extends from the peak altitude of the daytime E-region to the bottom side of the

55 *F*-region. As the behavior of the *ILs* is little discussed in the literature, and in order for the reader to become familiar with the subject that this paper is going to deal with, we will first present a brief summary of the main characteristics of the *ILs* over the equatorial and low latitudes sectors over Brazil, and then we will be able to understand how the magnetic activity can affect these layers.

Recently, dos Santos et al. (2019) and Santos et al. (2020; 2021) have studied the essential
60 characteristics of the *ILs* over the Brazilian sector during the minimum and the maximum solar activity epochs and observed that these layers are predominantly diurnal and present a typical downward movement that can last from minutes to hours. Depending on the height at which the *ILs* are formed, they can descend and merge with the normal ongoing sporadic -*E* (*Es*) layers. The *IL*s' occurrence over Brazil is high and seems to be dependent on the magnetic inclination angle and independent (or weakly
65 dependent) on the solar activity. Nocturnal *ILs* also were observed over Brazil. Regarding the shape in which the *ILs* are seen in the ionograms, it was verified that they presented a curved format similar to the "h" type *Es* layer, however the *ILs* with a straight format and spreading base appearance also were observed.

The studies conducted so far on the *ILs* over Brazil give us some indications that the dynamics of
70 these layers can be influenced by the atmospheric tides, gravity waves, and electric fields. The day-to-day variability in the average *ILs*' descent velocity also suggests the influence of a periodic perturbation with a periodicity of some days. The velocity values found are compatible with those of the semidiurnal and quarter-diurnal tides. However, the larger descending rate (> 10 km/h) observed over the equatorial region may reveal an additional influence of the gravity waves in *IL*'s dynamics. Additionally, Santos et
75 al. (2021) reported interesting events in which the *ILs* presented an upward movement at the same time in which the *F* layer rises due to the evening prereversal enhancement of the zonal electric field. Such characteristic was observed in most of the cases during a period of high solar activity, between October and April months, however a single case also was observed in 2009. Therefore, it is possible that the more intense zonal electric field in 2003 could have an important contribution to the upward movement of the
80 *ILs*. Another interesting characteristic observed in *ILs* is that the *ILs* could suffer in some way the influence of the prompt penetration electric fields. Dos Santos et al. (2019), for example, showed a case

3

in which a daytime *IL* over the equatorial region of São Luis (2ºS; 44ºW) on October 9, 2009 presented a strong upward movement that carried the *IL* to the base of the *F2* layer in ~ 1.5 hours. This anomalous rise was probably caused by the joint action of the atmospheric gravity wave propagation and the PPEF.

85 Santos et al. (2021) also reported the ascending ILs, however, during sunset times. As mentioned by the authors, it is possible that the *ILs* in these cases had been caused by the action of the PRE and in some events by an additional contribution from the prompt penetration electric fields. In all the events, the *ILs* were located at altitudes higher than or equal to 175 km, except the event of November 10, 2003, when an *Es* layer located at about 120 km of altitude presented an abrupt rise reaching 290 km of altitude in a

90 time interval of ~ 1.25 hours. This rapid rise of the *Es/IL* layers probably was caused by an eastward electric field of ~ 0.6 mV/m arising from the PRE and the PPEF (for more details, see Santos et al., 2021).

The focus of this paper is to investigate the geomagnetic activity effects on the intermediate layers over the Brazilian low latitude sector during the deep solar minimum of 2009. As mentioned previously, this epoch is especially suited to develop studies like the one proposed here due to the very low values of

95 the solar decimetric flux (10.7cm) that were observed. In this case, the effects caused in the *ILs* by the variability of radiation coming from the Sun can be neglected, and consider only those caused by geomagnetic variations. The data and methodology used to investigate the possible influence of the geomagnetic storms in the intermediate layers is given in Section 2. The results are presented in Section 3 and finally, in Section 4, the discussion and conclusions.

100 **2. Data set**

In this paper, the ionospheric sounding data collected by the Digisonde operated over the low latitude site, Cachoeira Paulista (CP, 22.42° S; 45° W, I: -34.4°), during the deep solar minimum of 2009 are used to verify the possible dependence of the *ILs* on the geomagnetic activity. The *ILs*' virtual height (*h'IL*) and top frequency (*ftIL*) are analyzed as a function of the Kp index. The *ILs* data were processed

105 using the SAO Explorer software (Reisnish, 1986) at each 15 minutes. All the observed *ILs* were included in the analysis, regardless of their descending or ascending movement.

Before going into detail on the topic that this work proposes, we will first give an overview of the behavior of *ILs* on the sector of CP. Figure 1 shows the variability of the parameter of frequency and

height of the *ILs* (panels **a** and **b**), their distribution with the local time (panel **c**), as well as their rate of

110   occurrence for different seasons of the year. The red, blue and gray colors are used to represent the summer (December solstice), winter (June solstice) and equinoxes, respectively. It can be observed that in general the *ILs* attain higher frequencies (> 6 MHz) after 11:00 LT (panel **a**) (except in some cases), and present a high variability in height during all the analyzed period. The downward movement of the *ILs* is one of the important characteristic that also can be observed in panel **b**. As indicated in panel **c**, the

115   occurrence of the *ILs* along the day is not continuous, which means that the *ILs* can appear and disappear many times during the day or simply not occur. Additionally, panel **c** also shows that in some periods (especially in winter, with some exceptions), there is a tendency that the *ILs* be formed a little later (after 08-09 LT). Regarding panel **d**, it can be seen that the *ILs* occurrence in the low latitude sector of CP increases significantly in the first hours of the day attaining its maximum at ~14:00 LT in summer, ~12:00

120   LT in winter, ~10:30 LT in the equinoxes. In general, the probability of occurrence decay drastically as the nighttime period approaches (Note: the seasons were equally divided, i.e., 121 days around the solstices and 61 days around the equinoxes).
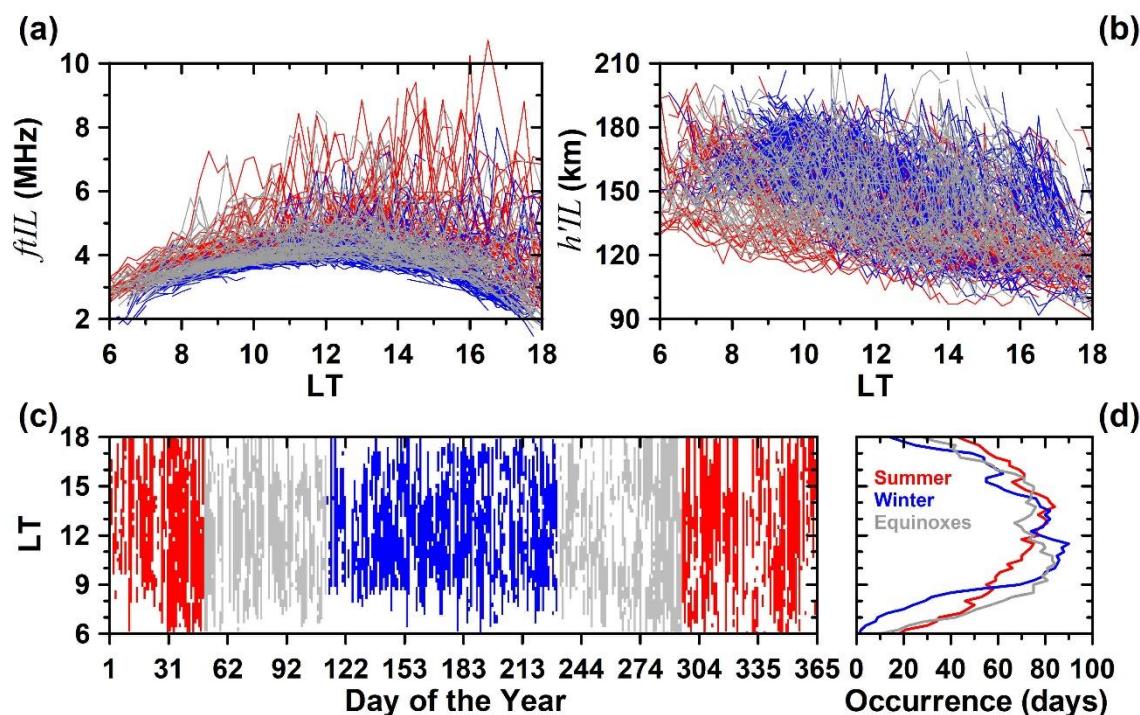
125

Figure 1: Behavior of the frequency (*ftIL*) and height (*h'IL*) parameters of the intermediate layers over Cachoeira Paulista during 2009 (panels a and b, respectively) in function of local time; distribution of the ILs occurrence with the local time in function of day of the year for 2009 (c), and; the seasonally occurrence probability of the *ILs*. In each panel, red, blue and gray are used to represent Summer, Winter and Equinoxes, respectively.

130   Figure 2 summarizes the geophysical condition of the data distribution according to the solar and geomagnetic activities based on the F10.7P index and Kp_{av} index, respectively. The F10.7P (gray line in top left panel) is a combination of the daily decimetric solar flux index (F10.7) and one more term (F10.7A), which corresponds to the average of the 81 previous days, thus F10.7P= (F10.7A + F10.7)/2 (given in Solar Flux Units (SFU); 1 SFU = 10^{-22}W/(m^2Hz)). F10.7P was chosen because several authors

135   have shown that the ionospheric parameters are better described by this index (Brum et al., 2011 and 2012; Goncharenko et al., 2013). In fact, Brum et al. (2011) and Brum et al. (2012) have shown that the best description of the UV-EUV (based on UV-EUV irradiance data from Pioneer Venus Orbiter (10– 150 nm) and by the Solar EUV Monitor onboard the Solar Heliospheric Observatory (26–34 nm and 0.1– 50 nm bands)) is given by F10.7P when compared with F10.7. In addition, their works have shown that

140   the UV-EUV emissions tend to increase with F10.7P until a certain threshold (around 175 SFU). However, for low solar activity, the UV-EUV variations with the F10.7P can be well represented by a linear function and this feature is very important for the methodology employed in this work, as seen below. The Kp_{av} (gray line in left bottom panel) is the average of the 3 hours data current Kp value and the previous 3 and 6 hours, that is, $Kp_{av} = (Kp_{(ref)} + Kp_{(ref-3)} + Kp_{(ref-6)})/3$, which gives the standard behavior

145   of the geomagnetic activity and avoid sharp gradients in the temporal edges of this index (every 3 hours). Then, in the case of Kp_{av}, different values can be defined per day, since the *ILs* can occur in different intervals of the day.

        The occurrence number in hours of the Kp_{av} level in this period is presented on the right bottom panel of Figure 2 (red bars). It is observed that all of the data were acquired during very low to normal

150   geomagnetic activity ($Kp_{av} \leq 3^+$ or 3.3) according to the Wrenn et al. (1987) classification. Such distribution is very similar to that found by Terra et al. (2020) when the authors analyzed the MSTID events for the period starting in the middle of 2018 to the end of 2019 (also low solar activity). Note that

the occurrence of various levels of magnetic activity is well distributed throughout the year (left bottom panel of Figure 2) and this behavior is the optimum condition for the kind of analysis of this work, as will

155 be seen in this report. Regarding the solar activity, the period that encompasses our dataset is the end of solar cycle #23 and the beginning of solar cycle #24. A growth of activity and fluctuations of F10.7P along the year is observed, varying from 66.5 SFU to 78.1 SFU (average of 70.1 SFU, top right panel) and an uneven distribution of F10.7P (left upper panel) may be noted. This was a period of very low solar activity in terms of solar flux irradiance (see Emmert et al., 2010) and many works have reported unusual

160 responses of the upper atmosphere/thermosphere under this condition. For instance, during this period, reduction of ionospheric temperatures and densities were detected over several latitudes (Coley et al., 2010; Heelis et al., 2009; Yue et al., 2010; Klenzing et al., 2011; Aponte et al. 2013). Comparing the thermospheric total mass density from the prolonged minimum in solar activity between cycles 23 and 24 with that of the previous solar minima, Emmert et al. (2010) detected a reduction of about 10–30%

165 compared with the climatologically expected levels. Heelis et al. (2009) and Aponte et al. (2013) reported an unprecedented contraction of the topside ionosphere to altitudes never reported before.
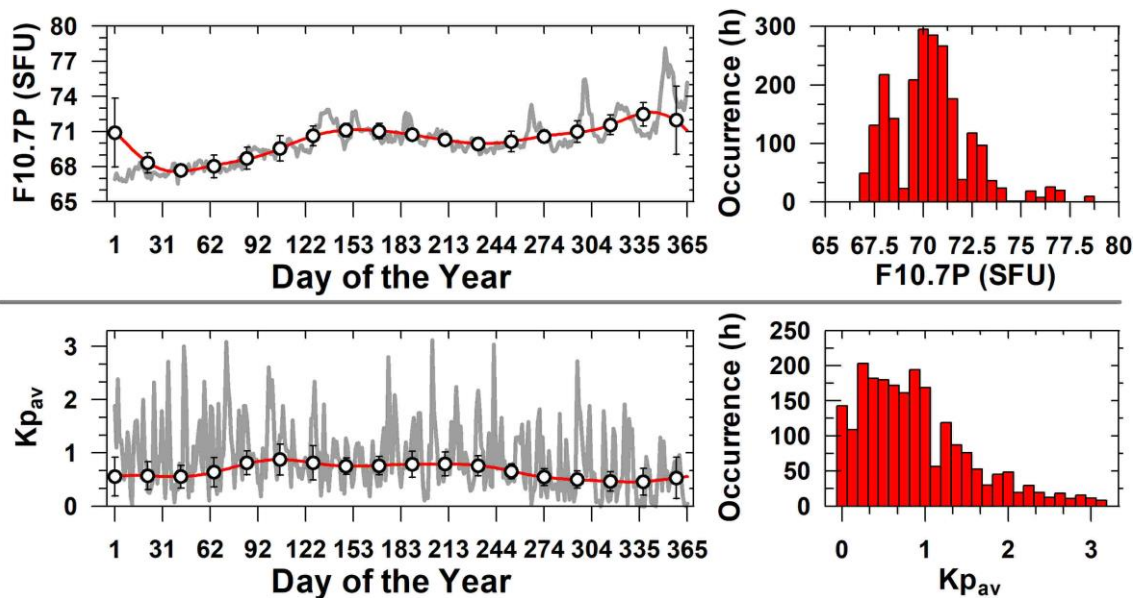
Figure 2: Variability of the solar and geomagnetic activity quantified by the F10.7P and the Kp_{av} indices (upper and bottom block of panels, respectively) for the studied period. Left panels show the geophysical conditions as a function of the day of the year while the right panels their corresponding number of occurrences (in hours) under different geophysical conditions. The dots of the left upper panel represent the 41 days averages and the standard deviation of F10.7P, while dots of the left bottom panel represent the same range of days of the upper panel and its respective standard deviation but for $Kp_{av} \leq 2.3$ (geomagnetic condition used to construct the quiet time condition of *h'IL* and *ftIL*) (Note: Left panels show the geophysical conditions as a function of the day of the year (gray line)). The red continuous lines are the reconstruction of these variabilities using Fast Fourier Transform (FFT). The given occurrence in the right column of panels is the number of hours for a given interval of Kp_{av} (0.125) and F10.7P (0.5 SFU).

In our study, it has been used the *h'IL* and *ftIL* parameters as obtained from the Digisonde observation over Cachoeira Paulista. From these data, an empirical climatological model was developed that accounted for the dependences of these parameters on time and season, under low solar and geomagnetic activities. Determining the variability of *ILs*' parameters in function of time and season make it possible the isolation of any changes related to geomagnetic activity. The first step in our

methodology was to extract the seasonal quiet time behavior of the *h'IL* and *ftIL* parameters. For this, it was employed the weighted arithmetic mean defined as $x(t_{ref}, d)$ represented as (equation 1):

$$\bar{x}_{(t_{ref}, d_{ref})} = \frac{\sum_{d_{ref}-20}^{d_{ref}+20}\left[x_{(t_{ref}, d)}(|d_{ref}-d|)\right]}{\sum_{d_{ref}-20}^{d_{ref}+20}(|d_{ref}-d|)} \tag{1}$$

190   where x denotes *h'IL* or *ftIL* values under the geomagnetic activity condition below $Kp_{av} \leq 2.3$ for the time reference t_{ref} and the selected day of the year (*d=DOY*). The average value of height and frequency of the *ILs* was calculated considering 20 days adjacent to the d_{ref} and 30 minutes around the t_{ref}.

From the quiet time variability of the *h'IL* and *ftIL* obtained by the 41 days weighted arithmetic mean process a simple model was built using finite Fourier series reconstruction following the procedure

195   by Souza et al. (2010) and Brum et al. (2011), given by

$$xV_{(t,d)} = A0_{(t)} + 2\sum_{m=1}^{4}\left[Am_{(t)}\cos(2\pi m f_1 d) + Bm_{(t)}\sin(2\pi m f_1 d)\right] \tag{2}$$

where $xV_{(t,d)}$ is the reconstructed variable as a function of time in LT *(t)* and DOY (*d*) (*xV* stands for *h'IL* or *ftIL*), f_1 is the fundamental frequency of the parameter to be reconstructed (1/365), $A0_{(t)}$ is the annual average of the such parameter for a given (*t*), and finally, $Am_{(t)}$ and $Bm_{(t)}$ are the mth Fourier coefficients

200   also as a function of time. The terms $A0_{(t)}$, $Am_{(t)}$ and $Bm_{(t)}$ were incorporated to the model using polynomial fittings in function of time (LT), as shown in Figure 3, for the harmonics m=1 (one year), m=2 (~6 months), m=3 (~4 months) and m=4 (~3 months). The upper left (*h'IL*) and right (*ftIL*) panels show the time dependence of $A0_{(t)}$ open circles for Fourier coefficients and continuous lines for adjustments). The values of $Am_{(t)}$ and $Bm_{(t)}$ are presented in the lower right and left panels by the blue

205   and red curves, respectively, white their best polynomial fitting as well.
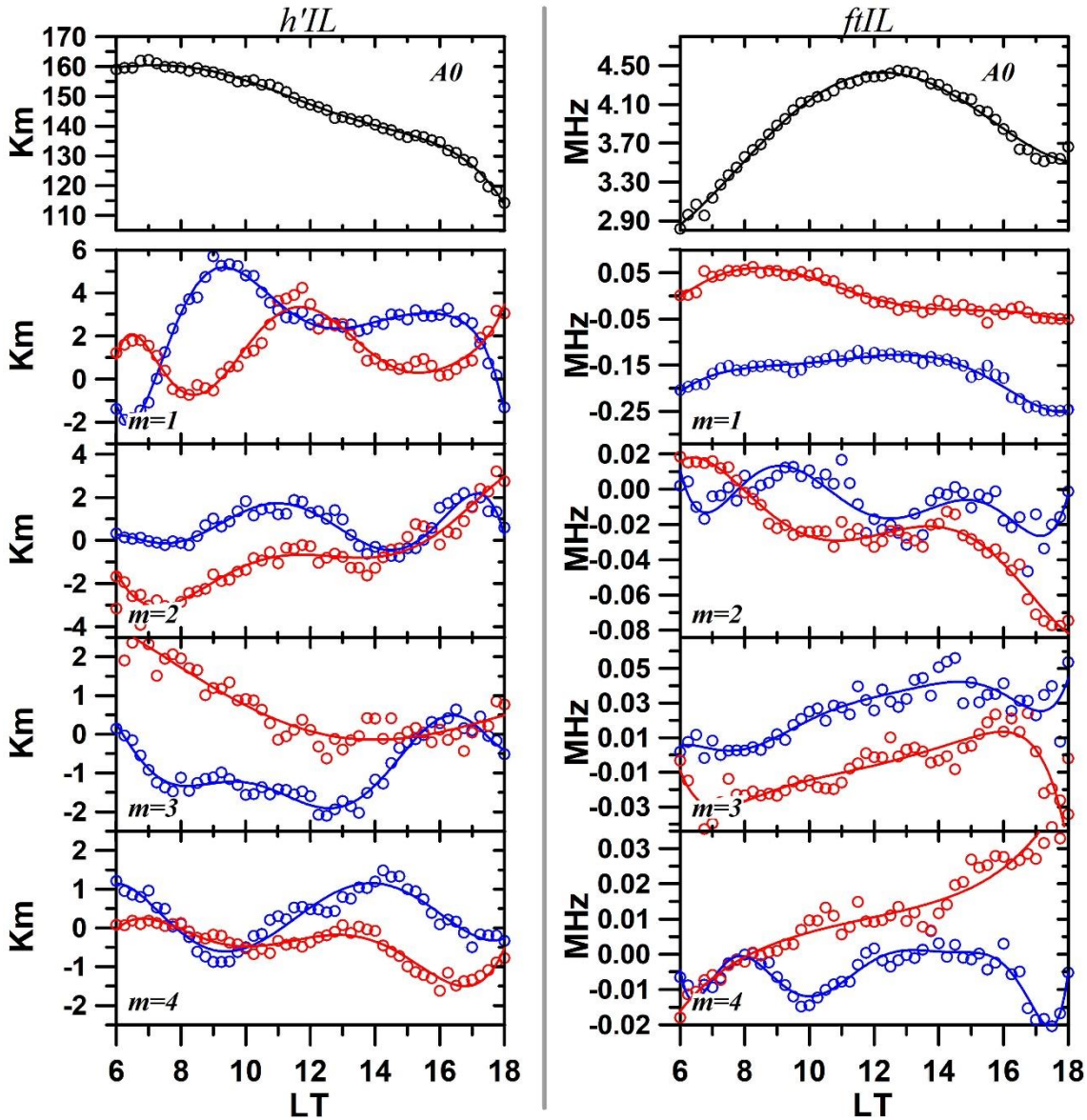
Figure 3: Dependence of the h'IL/ftIL's FFT coefficients as a function of LT (left/right, respectively). The circles are the values obtained by the FFT decomposition, while the continuous lines are the best polynomial approximation (more information in the manuscript body). The colors blue and red are used to represent the coefficients values of $Am_{(t)}$ and $Bm_{(t)}$, respectively.

Based on the model output above described, Figure 4 shows the behavior of the *h'IL* and *ftIL* during the year from 06:00 to 18:00 LT (top and bottom panel, respectively). The right panels show the dispersion diagram between the model and its respective weighted arithmetic mean (under $Kp_{av} <= 2.3$)

obtained by equation 1, wherein it is possible to see the good correlation between the observation and the

215 modeled data. The left panels show the dominance of the semi-annual and annual variation of the *ILs*'

virtual height and top frequency, respectively. It is interesting to observe that the upper intermediate layers

(>160 km) are formed as winter approaches in southern hemisphere between ~ 06:00 LT and 11:00 LT,

with a maximum in April/May (DOY 92-153) before the local noon. A second maximum is observed

from the begging of November to middle of January (DOY 304-15), however, in a more restricted range

220 of time (prior ~09:00 LT). After 12:00 LT, the *ILs* are generally located at altitudes at or below to 150

km. In addition, it is observed that the evolution of the *ILs* to altitudes below 120 km was more evident

between the months of April and May (DOY 92-153) at the end of the day. The bottom left panel shows

an annual variation of the top frequencies, with a maximum at about 12:00-13:00 LT from November to

February (DOY 304-62). It can be observed that the upper *ILs* present lower frequencies when compared

225 to the layers located near 150 km. As the ILs descend, they reach the E region and merge with the existing

Es layer, increasing in this way, the top frequency of the layer due to the presence of the metallic ions.
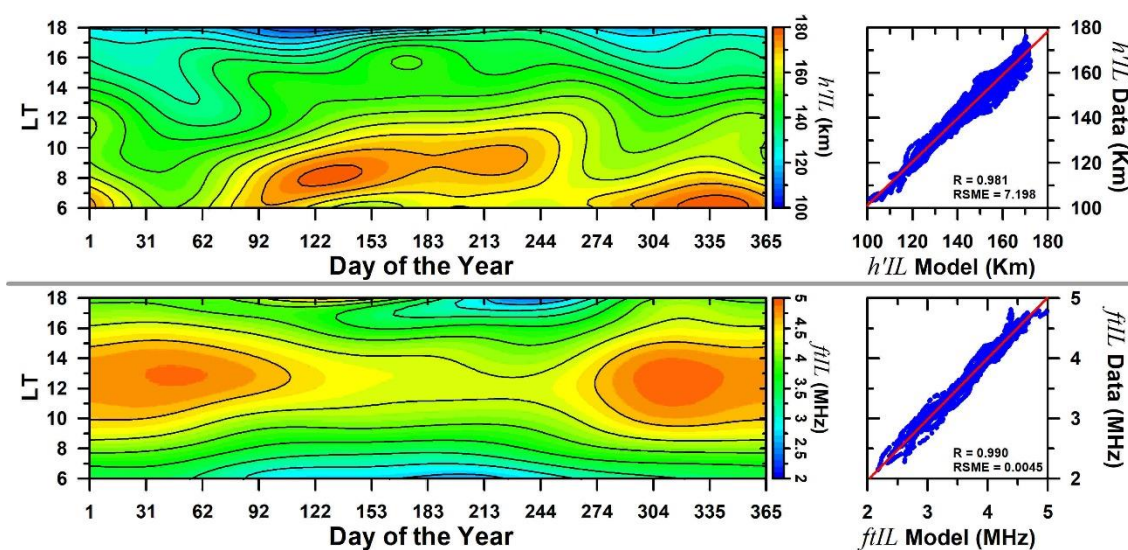
Figure 4: **Contour plot of the annual variation of the modeled virtual height (h'IL, left top panel) and top frequency (ftIL, left bottom panel) of the intermediate layers over Cachoeira Paulista. The dispersion diagrams on the right hand-side show the**

230 **correlation between the weighted arithmetic mean and model results. In each panel on the right, the Correlation Coefficient (R) and Root Mean Square Error (RSME) values are also provided.**

Figure 5 exemplify how the dependence of the different parameters of the intermediate layers in respect to geomagnetic activity was investigated in this work using ΔKp_{av}. The ΔKp_{av} is the mean of the respective Kp_{av} (gray line in the left bottom panel of Figure 2, $Kp_{av} = (Kp_{(ref)} + Kp_{(ref-3)} + Kp_{(ref-6)})/3$) minus the average of any value below $Kp_{av} <= 2.3$ in a range of ± 20 days (this is the geomagnetic condition that the model was developed, the red line shown in the left bottom panel of Figure 2). Noticed: The usage of the residuals minimizes the background quiet time behavior variation along the time (LT and season), enhancing this way the detection of the real contribution or not of the geomagnetic activity on the *IL*s parameters. The upper panel of Figure 5 shows the whole dataset sorted from the lowest to the highest ΔKp_{av} values and divided into eight sections with the same percentage of samples for each range of ΔKp_{av} (12.5%, represented by the black vertical lines) for the summer (December solstice) at 17:30 LT± 30 minutes. Specifically, for this example, the selected range represents 178 data points, i.e., each 12.5% displays the behavior of ~22 individual data samples. This panel also displays the respective F10.7P values (red line) and its respective average and standard deviation (blue open circles) for the same sorted 12.5% occurrence range of ΔKp_{av}. Note that the F10.7P mean variation for each range does not vary much which leads us to emphasize that the following variations of *ILs* are due to geomagnetic activity. The bottom panels show the *h'IL* and *ftIL* responses to the geomagnetic activity by the residual average obtained by the difference of the data and the model output presented in Figure 4 in function of ΔKp_{av}. The open circles represent the average values of the height/frequency residuals ($\Delta h'IL$ and $\Delta ftIL$, respectively) for the eight different levels of ΔKp_{av} and their respective standard deviations (vertical and horizontal lines). The linear fitting is indicated by the blue lines. The slope (SLP) of the dependence of *h'IL* and *ftIL* with respect to the geomagnetic activity variation (km. ΔKp^{-1} and MHz. ΔKp^{-1}) and the correlation factor (R) are also shown. In this example, it can be clearly observed that as the geomagnetic activity increase, the height of the intermediate layers also increases. The opposite occurs with the frequency when an increase of the Kp causes a decrease in this parameter.
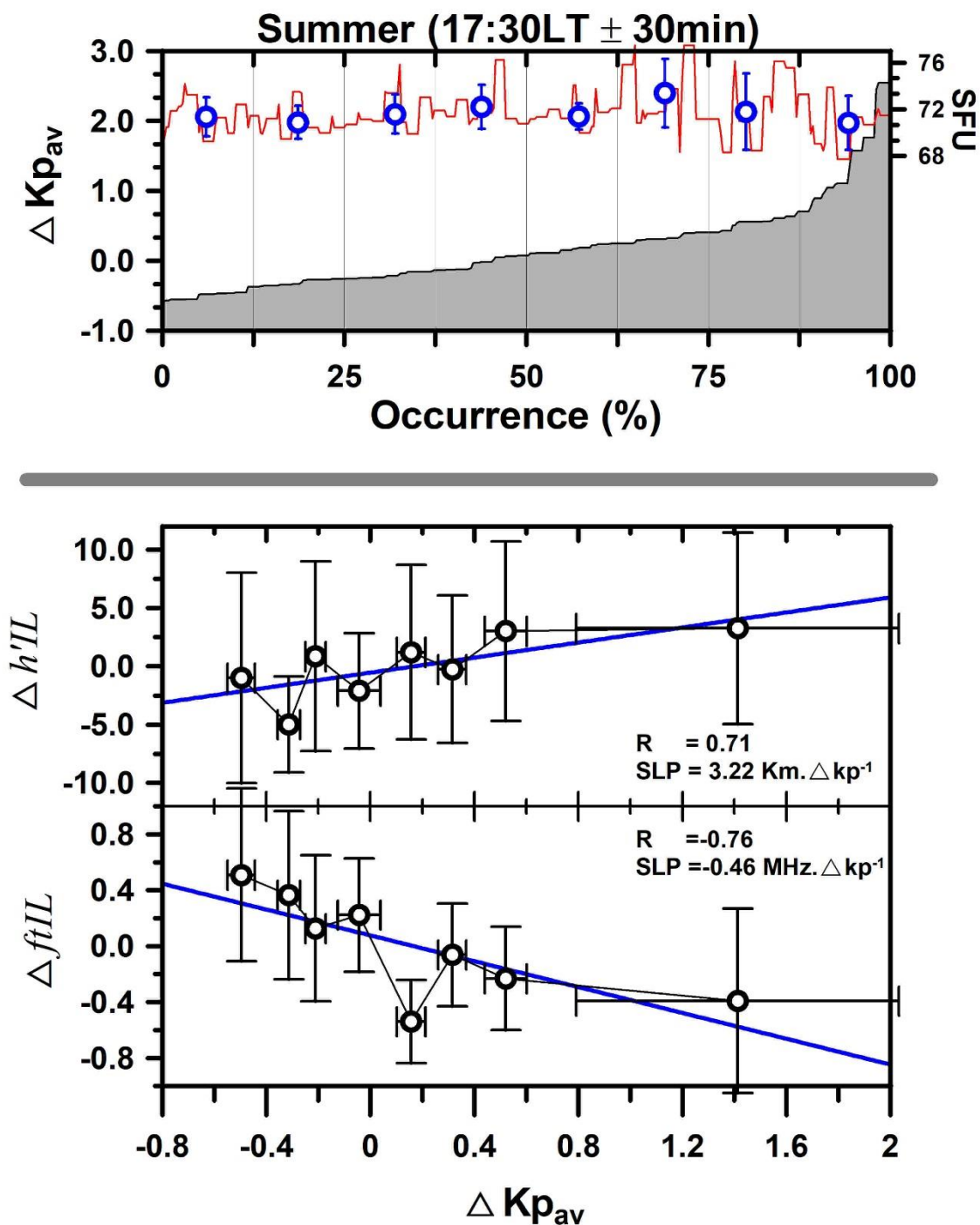
Figure 5: Responses of the intermediate layer to the geomagnetic activity for summer at 17:30 LT±30 minutes. The upper panel shows the ΔKpav (see more information in the text) data organized from the lowest to the highest values and divided into eight sections with the same percentage of samples. In addition, the values of F10.7P with respect to

ΔKpav and the average of the F10.7P (blue open circles) for each section are also presented. The bottom panels show the linear regression fitting over the height and frequency residual variability relative to the average ΔKpav values.

The same methodology explained in the case of Figure 5 was applied to all the data between 06:00 and 18:00 LT for each season. Due to the lack of data, the night period was excluded from our analysis.

265 Figure 6 shows the *ILs*' dependence on the geomagnetic activity in terms of height (first two columns from left to right) and frequency (two columns of the left) for different seasons of the year. The data were grouped in summer, equinoxes, and winter. The correlation coefficient (R) of both parameters is also shown at the right column of each block of panels. The variations of the geomagnetic activity presented in this figure were 2.13±0.28 (summer), 2.18±0.24 (equinoxes) and 1.72±0.21 (winter) in Kp index units.

270 It is observed that the higher variability in *ILs'* height with geomagnetic activity occurs during the summer period. In this case, the *IL* goes down fast with the increase of the geomagnetic activity in the beginning of the day. In the following hours, this descent decrease until a moment in which an opposite behavior occurs, that is, a small rise of the *IL* begins to be observed with the increase of the ΔKp_{av}. Although some fluctuation in the R-value can be observed (mainly during the equinox and winter), there is a tendency

275 that the *ILs*' height increase with the Δkp variation in all seasons after ~12:00 LT, as can be seen by the positive values of km.ΔKp^{-1}. Regarding the behavior of the frequency, it is noticed that in the summer, the *ftIL* parameter presented a tendency of increase with the geomagnetic activity in the beginning of the day (~ 0.1 MHz.ΔKp^{-1}), however from ~12:00 LT on there is a significant decrease in the *ftIL* with ΔKp_{av} (mainly after 16:00 LT) as can be confirmed by the negative values of the coefficient correlation (R).

280 During the equinox, the general tendency is that the *ftIL* decrease along the day, and during the winter, little or no response of the top frequency to ΔKp_{av} variability can be observed prior 16:00 LT and sharp decrease after the referred period similar to what is observed during the summer.
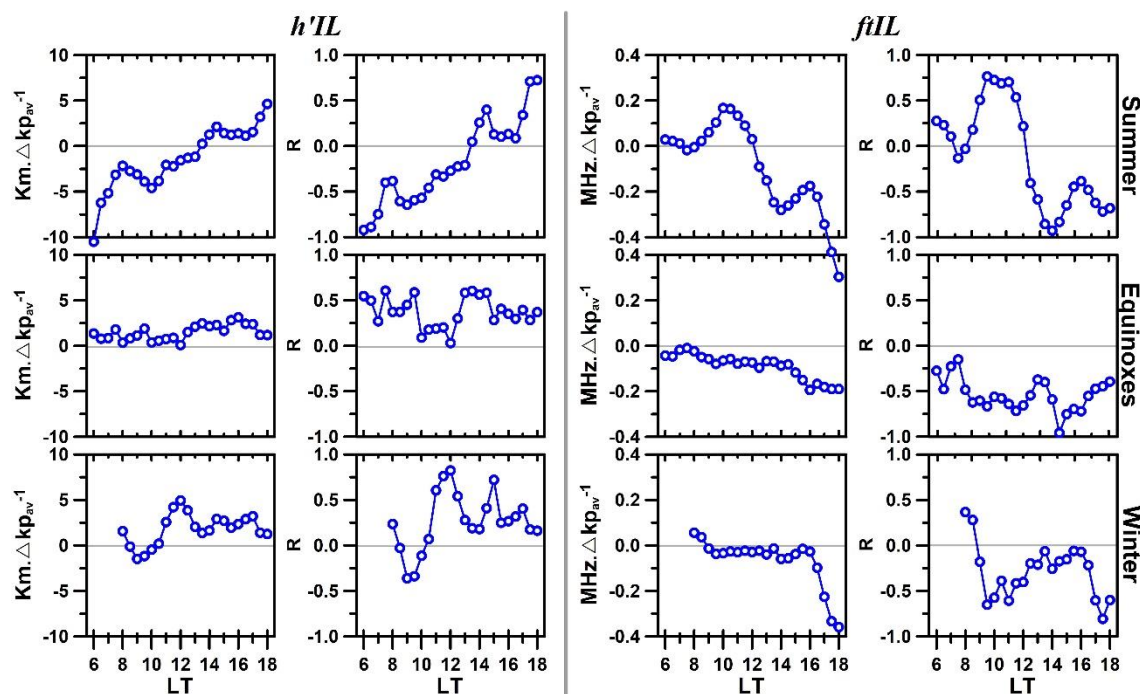
Figure 6: Geomagnetic activity effects on *h'IL* and *ftIL* parameters for different seasons. The first two panels (from left to right) show the linear regression of the *h'IL* as a function of the ΔKp_{av} index over the different times of the day and the correlation coefficient R. The two right panels indicate the same but for the *ftIL* parameter.

4. Discussion and Conclusions.

It is well known that geomagnetic activity can drastically modify the low-latitude ionospheric dynamics. During the last solar minimum, a unique opportunity was available to investigate such dynamics, since the effects of the solar activity, that dominates the temporal variability of ionospheric properties, could be practically disregarded due to very low solar radiation variation. Using Digisonde data from a Brazilian low latitude station, Cachoeira Paulista, we studied the impacts of the geomagnetic activity in the height and top frequency of the intermediate layers during the deep solar minimum of 2009.

The results summarized in Figure 6 revealed, for the first time, that the most expressive response of the *ILs* over the low latitude region of Brazil to the geomagnetic activity occurred during the early morning hours (~06:00 - 08:00 LT) of the summer when the *ILs* presented a trend of a rapid descent with the increase of the Kp_{av} (as indicated by the negative values of $km.\Delta Kp_{av}^{-1}$ in *h'IL* panels). It is possible

that this variation in the height of the *ILs* could have been caused by disturbance electric field having the nature of an over-shielding electric field such as that associated with the northward IMF Bz turning. Such

300   electric fields have westward polarity during daytime and therefore it may be one of the factors responsible for the descending movement of the intermediate layers at this time. As pointed out by Santos et al. (2021), depending on the height at which the *ILs* are located, the disturbance electric field can affect considerably the vertical displacement of the intermediate layers. They showed that the eastward PPEF can affect partially the rise of the *ILs* located at higher altitudes (> 170 km) at sunset times. As shown in

305   Figure 4 of the present work, the *ILs* were located at altitudes very close to this limit (> 165 km) between ~06:00 LT and 08:00 LT from October to January, reinforcing in this way the idea that a disturbance electric field could be responsible for the downward movement of the *ILs*.

Another interesting point that needs to be considered is that the movement of the *IL*s can also be influenced by the regular undisturbed day-to-day variations in the zonal electric field of the ionosphere

310   that is directed to east/west during the daytime/nighttime hours. Therefore, it is possible that in the first 2-3 hours of our analysis period, the descent of the IL could be a result of a competition between the eastward zonal electric field created by the *E*-region dynamo and the disturbance westward electric field arising from the *overshielding* process. In the following hours, the layer descent movement during the summer and winter slowed down until a moment in which an opposite situation was observed, that is, a

315   small rise of the *ILs* occurred in all seasonal periods analyzed, as denoted by the positive values of the rate km.ΔKp_{av}^{-1} in the first set of panels on the left in Figure 6. As mentioned by Santos et al. (2019), the rise of an *IL* during daytime can also be a result of the joint action of the of the eastward PPEF (*undershielding*) and gravity wave propagation. In the case studied by dos Santos et al. (2019), the rise of the *IL* also was accompanied by a decrease in their top frequency. Wakai (1967) reported that the height

320   of the intermediate layer over Boulder (40ºN; 105ºW) also can be influenced by the magnetic disturbances, however their observation was made during the nighttime.

At the same time in which a decrease in the *ILs* height is observed, an increase in the *ftIL* parameter occurs during the summer between 08:00 and 12:00 LT attaining a maximum of 0.2 MHz.ΔKp_{av}^{-1} at 09:00 LT. It is interesting to observe that before 12:00 LT for example, the rate variation of the *ftIL* was positive

Annales
Geophysicae
Discussions

325   indicating that during the downward movement, the *ILs*' top frequency increased from its initial value. This increase in the frequency is expected since as the layer descends, it can suffer an additional increase of ionization arising from the metallic ions that contribute to the ion density in the ongoing sporadic-E (*Es*) layers. As the *ILs* presented a rise after 13:00 LT, the tendency was that the *ftIL* decrease with the increase of ΔKp_{av}. Note that the after 16:00 LT, this decreased is more accentuated during the summer

330   and winter. Analyzing the incoherent scatter data from the mid-latitude region of Arecibo, Raizada et al. (2017) showed that the integrated electron content (*E*-region total electron content - ErTEC) between 80 and 150 km altitude regions presented a maximum variability throughout the night due to geomagnetic activity for both low and high solar activity during equinox periods. Besides that, the authors also verified that the integrated electron content during geomagnetically disturbed/normal conditions and high solar

335   flux periods displays positive changes during summer and equinox, while it is negative in winter. Wakai (1967) reported a study about the maximum electron concentration of the nighttime *E* layer, the valley above it, and the appearance of the intermediate layer from analysis of the low-frequency ionogram obtained at Boulder on three nights of quiet, moderate, and severe geomagnetic activity. They observed an increase of the ionization in the nighttime valley at times of increased magnetic activity and the

340   appearance of an intermediate layer in ~ 150 -160 km during periods of moderated activity.

       The effects of the magnetic storms on the intermediate layer were studied also by Rodger et al. (1981) using ionosonde data from South Georgia (54ºS; 34ºW). They showed that the rate of the downward movement and the final height of the nocturnal intermediate layer are independent of the season or magnetic activity. Additionally, they observed that the probability of formation of an *IL* when

345   the minimum virtual height of the *F2* layer is above 220 km is very low, but it can increase during magnetically disturbed periods. As shown by Santos et al. (2020), the *ILs*' occurrence over Cachoeira Paulista (22.42° S; 45° W) was very high both in 2009 (a low solar activity year and the same period of this report) and 2003 (a high solar activity year). These results show that in general, the *ILs* occurrence resulted to be independent of the magnetic disturbances, since the referred two periods of geomagnetic

350   activity are totally different from each other. However, their development/dynamics over Brazilian sector can be affected by disturbed electric fields, as shown by the results here presented and others previous publications (dos Santos et al. 2019 and Santos et al. 2021).

Although the impacts of the geomagnetic activity on different layers of the ionosphere have been extensively studied, there is a lack of information about what happens in the ionospheric valley region during such conditions, mainly over the low and equatorial latitudes. Using the low-power VHF radar data over the equatorial site of Jicamarca, Chau and Kudeki (2006) showed that the 150-km echoes were not affected by the electric field reversal caused by a magnetic disturbance (Kp=5). As mentioned by them, a statistical study on the *ILs* occurrence based on the magnetic activity index Kp did not identify any correlation between magnetic activity and the 150-km echoes. On the other hand, our results show that a small variation in Kp_{av} index (~ 2.0) can affect the *ILs*, especially in the morning period of the summer and late afternoon of all season over the low latitude sector over Brazil. Although the techniques used by us are different from those used by Chau and Kudeki (2006), the contrasting result reveals that the ionospheric valley is a complex region and additional studies need to be performed to understand the physical mechanism governing the generation of the intermediate layers during the occurrence of magnetic disturbances. It is important to emphasize that for the first time it was shown that a small variation in Kp_{av} index (by ~ 2.0) was able to impact the dynamics of the intermediate layer over the low latitude region during the period of deep solar minimum. The main results of this work are summarized below:

1. A small variation in the geomagnetic activity during low solar activity can affect both the parameter of height and frequency of the ILs over the low latitude Brazilian sector;

2. During the summer, the height of the ILs suffered a significant decrease with the increase of the magnetic activity magnetic in the first hours of the day. This characteristic was probably caused by an overshielding electric field;

3. During daytime, the smoothed rise of the ILs can be related to the regular day-to-day undisturbed zonal electric field of the ionosphere;

4. After 12:00 LT, there is a tendency that the frequency of the ILs decrease as magnetic disturbances increases, being this characteristic more intense after 16:00 LT, excepted in the equinox, when little or no response was found during all the interval analyzed;

5. A semi-annual and annual variation was observed in parameters of height and top frequency of the ILs, respectively.

References.

Balan, N., C. Y. Chen, J. Y. Liu, and G. J. Bailey (2012), Behavior of the low latitude ionosphere-thermosphere system at long deep solar minimum, Indian J. Radio Space Phys., 41, 89– 97.

Brum, C. G. M., F. S. Rodrigues, P. T. dos Santos, A. C. Matta, N. Aponte, S. A. Gonzalez, and E. Robles (2011), A modeling study of foF2 and hmF2 parameters measured by the Arecibo incoherent scatter radar and comparison with IRI model predictions for solar cycles 21, 22, and 23, J. Geophys. Res., 116, A03324, doi:10.1029/2010JA015727.

Brum, C. G. M., C. A. Tepley, J. T. Fentzke, E. Robles, P. T. dos Santos, and S. A. Gonzalez (2012), Long-term changes in the thermospheric neutral winds over Arecibo: Climatology based on over three decades of Fabry-Perot observations, J. Geophys. Res., 117, A00H14, doi:10.1029/2011JA016458.

Chau, J. L. and Kudeki, E.: Statistics of 150-km echoes over Jicamarca based on low-power VHF observations, Ann. Geophys., 24, 1305–1310, https://doi.org/10.5194/angeo-24-1305-2006, 2006.

Coley, W. R., R. A. Heelis, M. R. Hairston, G. D. Earle, M. D. Perdue, R. A. Power, L. L. H. B. J. Holt, and C. R. Lippincott (2010), Ion temperature and density relationships measured by CINDI from the C/NOFS spacecraft during solar minimum, J. Geophys. Res., 115, A02313, doi:10.1029/2009JA014665.

Dos Santos, Â. M., Batista, I. S., Abdu, M. A., Sobral, J. H. A., Souza, J. R., & Brum, C. G. M. (2019). Climatology of intermediate descending layers (or 150 km echoes) over the equatorial and low-latitude regions of Brazil during the deep solar minimum of 2009. Annales Geophysicae, 37(6), 1005–1024. https://doi.org/10.5194/angeo-37-1005-2019.

Echer, E., B. T. Tsurutani, and W. D. Gonzalez (2012), Extremely low geomagnetic activity during the recent deep solar cycle minimum, Proc. Int. Astron. Union, 7, 200– 209, doi:10.1017/S174392131200484X.

Emmert, J. T., J. L. Lean, and J. M. Picone (2010), Record-low thermospheric density during the 2008 solar minimum, Geophys. Res. Lett., 37, L12102, doi:10.1029/2010GL043671.

Goncharenko, L. P., V.W. Hsu, C. G. M. Brum, S.-R. Zhang, and J. T. Fentzke (2013), Wave signatures in the midlatitude ionosphere during a sudden stratospheric warming of January 2010, J. Geophys. Res.: Space Physics, 118, doi:10.1029/2012JA018251.

Hady, A. A. (2013), Deep solar minimum and global climate changes. Journal of Advanced Research, V4, I3, P.209-214. doi:10.1016/j.jare.2012.11.001.

Heelis, R. A., W. R. Coley, A. G. Burrell, M. R. Hairston, G. D. Earle, M. D. Perdue, R. A. Power, L. L. H. B. J. Holt, and C. R. Lippincott (2009), Behavior of the O+/H+ transition height during the extreme solar minimum of 2008, Geophys. Res. Lett., 36, L00C03, doi:10.1029/2009GL038652.

Klenzing, J., F. A. Simoes, S. Ivanov, R. A. Heelis, D. Bilitza, R. F. Pfaff, and D. Rowland (2011), Topside equatorial ionospheric density and composition during and after extreme solar minimum, J. Geophys. Res., 116, A12330, doi:10.1029/2011JA017213.

Kutiev I, Tsagouri I, Perrone L, Pancheva D, Mukhtarov P, Mikhailov A, Lastovicka J, Jakowski N, Buresova D, Blanch E, Andonov B, Altadill D, Magdaleno S, Parisi M & Miquel Torta J (2013), Solar activity impact on the Earth's upper atmosphere. J.Space Weather Space Clim., 3, A06, doi:10.1051/swsc/2013028.

Liu, J., L. Liu, B. Zhao, Y. Wei, L. Hu, and B. Xiong (2012), High-speed stream impacts on the equatorial ionization anomaly region during the deep solar minimum year 2008, J. Geophys. Res., 117, A10304,

Raizada, S.; Brum, C.G.M.; D. Mathews, J.D; Gonzalez, C; Franco, E. (2017). Characteristics of nighttime E-region over Arecibo: Dependence on solar flux and geomagnetic variations, Advances in Space Research, Volume 61, Issue 7, Pages 1850-1857, https://doi.org/10.1016/j.asr.2017.07.006.

Reinisch, B. W.: New techniques in ground-based ionospheric sounding and studies, Radio Sci., 21, 331–341, 1986.

Rodger, A. S., Fitzgerald, P. H., and Broom, S. M.: The nocturnal intermediate layer over South Georgia, J. Atmos. Terr. Phys., 43,1043–1050, 1981.

Santos, A. M., M. A. Abdu, J. R. Souza, J. H. A. Sobral, and I. S. Batista (2016), Disturbance zonal and vertical plasma drifts in the Peruvian sector during solar minimum phases, J. Geophys. Res. Space Physics, 121, doi:10.1002/2015JA022146.

Santos, A. M., Batista, I. S., Sobral, J. H. A., Brum, C. G. M., Abdu, M. A., & Souza, J. R. (2020). Some differences in the dynamics of the intermediate descending layers observed during periods of maximum

455   and minimum solar flux. Journal of Geophysical Research: Space Physics, 125, e2019JA027682.
       https://doi.org/10.1029/2019JA027682.

Santos, Â. M., Batista, I. S., Brum, C. G. M., Sobral, J. H. A., Abdu, M. A., Souza, J. R., &. (2021). F
       region electric field effects on the intermediate layer dynamics during the evening prereversal
       enhancement at equatorial region over Brazil. Journal of Geophysical Research: Space Physics.

460   Scherliess, L., and B. G. Fejer (1997), Storm time dependence of equatorial disturbance dynamo zonal
       electric fields, J. Geophys. Res., 102, 24,037–24,046, doi:10.1029/97JA02165.

Souza, J.R., Brum, C.G.M., Abdu, M.A., Batista, I.S., Asevedo, W.D., Bailey, G.J., Bittencourt, J.A.
       (2010), Parameterized Regional Ionospheric Model and a comparison of its results with experimental
       data   and   IRI   representations,   Advances   in   Space   Research,   46,   1032-1038,
465   https://doi.org/10.1016/j.asr.2009.11.025.

Sreeja, V., T. K. Pant, L. Jose, and S. Ravindran (2011), Westward electric field penetration to the dayside
       equatorial ionosphere during the main phase of the geomagnetic storm on 22 July 2009, J. Geophys.
       Res., 116, A03303, doi:10.1029/2010JA016013.

Terra, P., Vargas, F., Brum, C. G. M., & Miller, E. S. (2020). Geomagnetic and solar dependency of
470   MSTIDs occurrence rate: A climatology based on airglow observations from the Arecibo Observatory
       ROF.   Journal   of   Geophysical   Research: Space   Physics,   125,   e2019JA027770.
       https://doi.org/10.1029/2019JA027770

Zerbo J.L., Amory-Mazaudier C., Ouattara F., 2013. Geomagnetism during solar cycle 23:
       Characteristics. J. Adv. Res, 4(3), 265–274. doi:10.1016/j.jare.2013.08.010.

475   Wakai, N. (1967), Quiet and disturbed structure and variations of the nighttime E-region, J. Geophys.
       Res.,72, 4507-4517.

Wrenn, G., Rodger, A. S., & Rishbeth, H. (1987). Geomagnetic storms in the Antarctic F-region. I.
       Diurnal and seasonal patterns for main phase effects. Journal of Atmospheric and Solar-Terrestrial
       Physics, 49(9), 901–913. https://doi.org/10.1016/0021-9169(87)90004-3

480 Yue, X., W. S. Schreiner, J. Lei, C. Rocken, Y. Kuo, and W. Wan (2010), Climatology of ionospheric
upper transition height derived from COSMIC satellites during the solar minimum of 2008, J. Atmos.
Terr. Phys., 72, 1270–1274, doi:10.1016/j.jastp.2010.08.018.

485